Second IEEE Conference on Control Applications, September 13 - 16, 1993 Vancouver, B.C.

Robust Control Design for a Conventional Series Resonant Converter using μ-Synthesis

Zi-Qin Wang[†], Mario Sznaier[†], Issa Batarseh[‡] and Junyu Bu[†]

[†] Electrical Engineering, Pennsylvania State University
University Park, PA 16802
[‡] Electrical Engineering, University of Central Florida
Orlando, FL 32816-2450

Abstract Because of their reduced switching losses, dc-to-dc resonant converters have been used extensively in the design of smaller size and lighter weight power supplies. The steady state and dynamic behaviors of both the conventional series and parallel resonant converters have been thoroughly analyzed and small-signal models around given nominal operating points have been obtained. These models have been used in the past to design controllers that attempted to keep the output voltage constant in the presence of input perturbations. However, these controllers did not take into account neither load nor components variations, and this could lead to instability in the face of component or load changes. Moreover, prediction of the frequency range for stability was done a posteriori, either experimentally or by a trial and error approach.

In this paper we use μ-synthesis to design a robust controller for a series resonant converter. In addition to robust stability the design objectives include rejection of disturbances at the converter input while keeping the control input and the settling time within values compatibles with a practical implementation.

1 Introduction

Because of their reduced switching losses, dc-to-dc resonant converters have been used extensively in the design of smaller size and lighter weight power supplies [1][2]. In resonant converters, the capacitor voltage and current waveforms exhibit sinusoidal behavior, allowing for the use of high operating frequencies. These high frequencies are desirable since they result in smaller, lighter magnetic components and faster transient responsed. In fact, today's dc-to-dc resonant converters have their operating frequencies well in the megahertz range [3]. As an additional advantage, the harmonic contents in resonant converters are much lower than those in Pulse Width Modulation converters.

Because of these features, high frequency resonant converters are currently the object of widespread interest and are rapidly becoming the preferred choice in applications requiring high-efficiency, high-density, dc-to-dc power converters.

The steady state and dynamic behaviors of both the conventional series and parallel resonant converters have been thoroughly analyzed [4] [5]. By using perturbation methods, small signal models around given nominal operating points have been obtained and used in the design of controllers that attempt to keep the output voltage constant in the presence of input perturbations. However, these controllers did not take into account neither load nor components variations. Moreover, prediction of the frequency range for stability was done a posteriori, either experimentally or by a trial and error approach.

In this paper we use μ-synthesis [6] to design a robust controller for a series resonant converter (SRC). The design objective is to robustly reject input variations in the presence of load and component uncertainty, while keeping both small control actions and settling times. This is accomplished by selecting appropriate weight functions reflecting these requirements.

The paper is organized as follows: In section 2 we briefly describe the Conventional Series Resonant Converter (SRC) and we provide a small signal model around a nominal operating point. In section 3 we analyze the characteristics of the plant. This analysis provides some insight into the nature of the control problem, in particular displaying the relatively poor control characteristics of the plant. In section 4 we indicate how to select the uncertainty weight to cover all the possible plants and how to select the performance weights to reflect the desired time-domain specifications and we use μ-synthesis to design a robust controller. Finally, in section 5 we provide simulation results showing the performance of the closed-loop system under different conditions.

2 Problem Description

2.1 The Conventional Series Resonant Converter[4]

The conventional series resonant converter circuit diagram is shown in Figure 1. The series resonant circuit consists of the inductor L and the capacitor C. The parallel combinations of the transistors and the diodes form bidirectional switches which operate at fifty percent duty ratio to generate a symmetrical square wave voltage, with frequency f_s, applied across the resonant circuit. The resonant inductor current is coupled to the output circuit using a full wave rectifier. The output capacitor

CH3243-3/93/0000-0885 $1.00 © 1993 IEEE

C_o behaves as a constant voltage sink in the steady state and is much larger than the resonant capacitor C. Finally, the resistor R_o and the voltages V_g and V_o represent the load, the line (input) and the output, respectively.

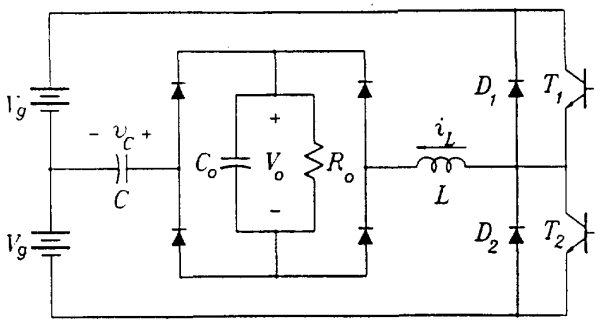

Figure 1: The conventional SRC circuit diagram

The nominal parameters used here are the same as the data in Chapter 3 of [4], i.e.

$L = 0.1335mH$;
$C = 12.8nF$;
$C_o = 32\mu F$;
$R_o = 19\Omega$;
$V_g = 40V$;
$V_o = 15V$;
$f_s = 100.35kHz$.

The following normalized variables are often used instead:

$V_{ng} = V_g/V_g = 1$;
$V_{no} = V_o/V_g = 0.375$;
$F_{ns} = f_s/f_o$.

where $f_o = \frac{1}{2\pi\sqrt{LC}}$ is the resonant frequency. It should be noted that the normalized output V_{no} is the same as the converter gain. Another useful parameter is the load condition $Q = \sqrt{\frac{L}{C}}/R_o$.

2.2 Small Signal Model

Under steady–state conditions, it can be shown [4] that there are four circuit modes in a switching period for the SRC operating in the continuous conduction mode. Thus the converter is a nonlinear, variable structure system, with its steady state state-trajectory uniquely determined by the normalized switching frequency F_{ns} and load condition Q. For a given operating point, a small signal discrete–time model of the converter can be obtained by using a perturbation method [4]. The sampling time for this discrete time model is equal to $T_s/2$, where $T_s = 1/f_s$ is the switching period. Therefore, due to aliasing effects, this model is correct up to the operating switching frequency.

The discrete model from the the normalized switching frequency F_{ns} and the normalized line V_{ng} to the normalized output V_{no} (to simplify the notation, we use the same variables for both the steady state and its perturbation) at the nominal operating point is given by the following state space realization [4]:

$$A = \begin{pmatrix} 0.7107 & 0.9449 & -2.5271 \\ -0.4335 & 0.6742 & -0.4008 \\ 0.0006 & 0.0011 & 0.9905 \end{pmatrix},$$

$$B = \begin{pmatrix} -4.1482 & 0.6637 \\ 10.6373 & 1.6742 \\ -0.0005 & 0.0008 \end{pmatrix},$$

$$C = (0 \quad 0 \quad 1)$$

2.3 Control Objectives

The purpose of feedback control is to keep the output voltage at a prescribed level (in our case $V_o = 15V$, i.e. $V_{no} = 0.375$) at all operating points, using as control input the switching frequency f_s. This problem can further be divided into three parts:

a. Line Regulation: The line voltage is often unregulated and could have a wide range of variation. This variation will be modeled as an external disturbance, thus leading to a disturbance rejection problem.

b. Load Regulation: On the other hand, the load condition could also vary over a wide range. Since the load R_o enters the dynamics of the model, load variations will appear as model uncertainty and could possibly lead to stability problems.

c. In addition to steady state requirements, we also need to have satisfactory transient responses under line voltage variation and (or) load change within the whole operating range.

Finally, in order to guarantee implementability of the resulting controller, all physical variables such as control input must be limited to practical values. Since these control objectives must be achieved for all possible values of the components and all load conditions, this constitutes in fact a robust performance problem.

3 Analysis of the Plant

To gain an essential understanding of the problem, we proceed with an analysis of the plant before designing a controller.

3.1 Control Characteristics

In the steady state, if any two of the variables among the normalized output V_{no}, switching frequency ratio F_{ns} and output load Q are specified, the third variable can be determined. The effects of the switching frequency and the load upon the converter output can be easily visualized by using this relationship, known as the control characteristics. From the control point of view, the control characteristics allows us to make a initial estimate of the load change that can be tolerated and see some of the difficulties in load regulation.

The control characteristics curves for various output loads Q are shown in Figure 2. As pointed out in [4], we see that the SRC has a relatively poor control characteristics. Since different control characteristics curves are far apart, a wide range of switching frequencies is needed to accomodate load changes. This further implies that the plant dynamics may vary significantly as the operating point changes. In this paper, the operating point varies along the dotted line in Figure 2 where the mark x indicates the nominal operating point.

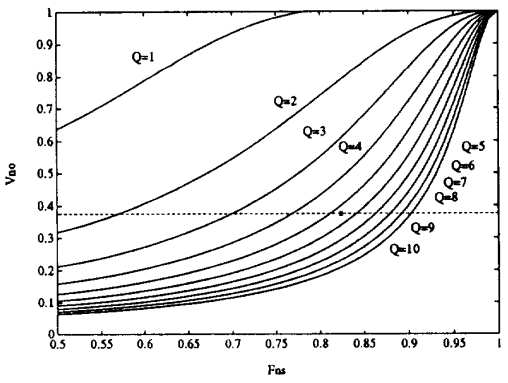

Figure 2: The conventional SRC control characteristics curves

3.2 Frequency Responses

From the discrete time state space model, we can easily get the z-transfer functions from the normalized switching frequency and the normalized line input to the normalized output

$$(\, G(z) \quad G_g(z)\,) = (\,0 \quad 0 \quad 1\,)[zI - A]^{-1}B \tag{1}$$

Finally, a transfer function in the frequency domain s can be obtained by using the bilinear transformation:

$$z = \frac{1 + sT_s/4}{1 - sT_s/4} \tag{2}$$

To simplify notation, we still use G and G_g to represent the nominal transfer functions in s. We have

$$G(s) = \frac{1.545 * 10^{-3}(s + 447980)(s - 362050)(s - 401400)}{(s + 1747.4)(s + 13443 - 157260i)(s + 13443 + 157260i)} \tag{3}$$

$$G_g(s) = \frac{8.207 * 10^{-5}(s + 267090)(s - 1874400)(s - 401400)}{(s + 1747.4)(s + 13443 - 157260i)(s + 13443 + 157260i)} \tag{4}$$

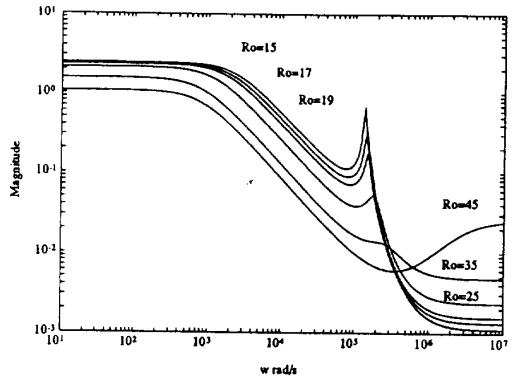

Figure 3: Frequency responses G(s) at different load conditions

The magnitude frequency responses $G(s)$ at nominal operating point as well as a few other load conditions are shown in Figure 3. At the nominal operating point, the converter has one real pole at -1747.4 and a pair of conjugate poles at $-13443 \pm 157260i$, responsible for the overshoot in the frequency response. As the load becomes lighter (i.e. load resistance R_o increases), the conjugate poles move farther to the left, with the overshoot decreasing, until they change into two real poles. If the load is decreased further, one of the real poles moves very fast towards $-\infty$ and then at $R_o = 47.1\Omega$ from $-\infty$ to $+\infty$, yielding an unstable open-loop plant. At this point, the perturbation technique used to obtain the small-signal model ceases to be valid. Therefore, in this paper, we limit R_o to be less than 45Ω. On the other hand when the load becomes heavier, the conjugate poles move towards the imaginary axis, resulting in increased overshoot. As we explain in detail latter, this results in a more difficult control problem.

4 Control Design

4.1 Structured singular value and μ-synthesis

Consider the standard 'M-Δ' structure shown in Figure 4, where M is a compatible matrix and $\Delta = diag\{\Delta_i\}$ represents a model perturbation with a block diagonal structure. The structured singular value μ is defined as [7]:

$$\mu_{\Delta}^{-1}(M) = \min_{\Delta}\{\bar{\sigma}(\Delta) | det(I + M\Delta) = 0\} \tag{5}$$

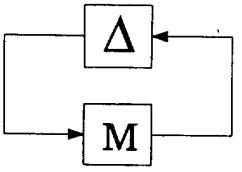

Figure 4: Standard "M-Δ" structure

As shown in [7], if M is a stable transfer matrix, a necessary and sufficient condition for robust stability of the interconnected systems for all perturbations $\|\Delta\|_\infty \leq 1$ is that $\mu(M) < 1$. Robust performance can be addressed by introducing an additional fictitious perturbation block. It can be shown [7] that *robust performance* is achieved if and only if:

$$\mu_{RP} = \sup_{\omega} \mu_{\Delta}(M) < 1 \tag{6}$$

where Δ contains now both the uncertainty and the performance blocks. The problem of finding a stabilizing controller which minimizes μ_{RP}, (μ-synthesis), is not fully solved yet. The present μ synthesis algorithm, called D-K iteration, is a combination of H_∞ synthesis and the optimal D-scaling. Although global convergence is not theoretically guaranteed, the algorithm works well in practice.

4.2 Uncertainty Weight Selection[9][10]

In this paper we use a single norm bounded multiplicative complex perturbation to cover all the possible plants. There are a number of uncertainty sources in the converter modelling. Load variation is, of course, a primary source. In this paper we assume that R_o is within the range from 17Ω to 45Ω which corresponds to Q within the range from 2.2695 to 6.0074. The Q value at nominal operating point is 5.375. Let $G^{R_o}(s)$ denote the transfer function from control input F_{ns} to output V_{no} at operating points $R_O \neq 19\Omega$. Then the multiplicative uncertainty can be expressed as

$$l^{R_o}(w) = |(G^{R_o} - G)G^{-1}| \tag{7}$$

Some sample uncertainties for different load R_o are shown in Figure 5. We can see that the multiplicative uncertainties have a peak in the oscillating frequency. This peak becomes larger and steeper as the load resistance R_o decreases. Covering this steep peak by a reasonable rational uncertainty weight, will inevitably introduce too much conservatism. This explains partially why in the electronics community, the SRC control systems are designed on the heaviest load.

Additionally, there might be some uncertainties in the resonant inductor L and capacitor C. Since they will result in a change of the load condition Q, they effectively behave as a load resistance R_o change. Hence we do not consider these uncertainties separately. Other uncertainty sources are neglected high frequency dynamics and limitation of the small signal modelling approach. Since these are primarily high frequency uncertainties, it follows that the uncertainty weight needs to be sufficiently large at high frequencies.

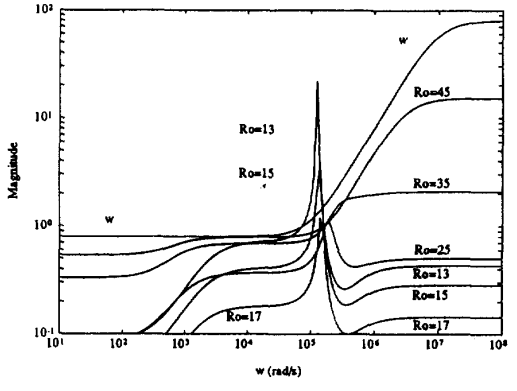

Figure 5: Multiplicative uncertainty for different load R_0 and uncertainty weight

The following multiplicative uncertainty weight is chosen for control design:

$$w_I(s) = 0.8\frac{10^{-5}s + 1}{10^{-7}s + 1} \tag{8}$$

The magnitude frequency response of $w_I(s)$ is also shown in Figure 5. It begins to increase at frequency $\omega = 10^5 rad/s$ and does not stop until reaching 80 at frequency $\omega = 10^7 rad/s$, thus covering both, high frequency uncertainties and all the uncertainties due to load changes from 17Ω to 45Ω. The relatively large magnitude (0.8) at low frequencies is due to the wide range of operating points, which results in a significant change in static gain. It should be pointed out that static gain change never leads to disk-like uncertainty at low frequencies because phase does not change much at low frequencies. Hence, this approach is potentially conservative since allows for uncertainties than will never appear in practice. To exclude these unexisting uncertainties, real μ may be used. However, as pointed out in [10], H_∞-norm and μ are worst case performance measures. Since robustness depends only on the *worst* uncertainty, introducing these additional uncertainties will not necessarily yield a more conservative design, which seems to be the case here. For example, we can improve the uncertainty modelling by use the following uncertainty weight

$$w_I'(s) = 0.5\frac{(0.016s + 1)(10^{-5}s + 1)}{(0.001s + 1)(10^{-7}s + 1)} \tag{9}$$

which has the same magnitude as $w_I(s)$ at middle and high frequencies but reduces the magnitude from 0.8 to 0.5 at low frequencies. However we found that this improved modelling made little difference in the performance of the closed-loop system.

4.3 Performance Weight Selection[8]

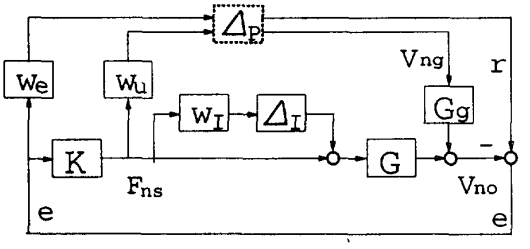

Figure 6: The block diagram for μ-synthesis

Figure 6 shows the block diagram used for μ-synthesis. Here Δ_I and ω_I represent the model uncertainty and its weight respectively. Δ_p, $\omega_e(s)$, and $\omega_u(s)$ represent the fictitious uncertainty block associated with the performance specifications and the performance weights associated with the tracking/regulation error and the control effort respectively. Although regulation is our primary concern, the reference input r is also included in our problem setting to get a reasonable design. The selection of $w_e(s)$ and $w_u(s)$ entails a trade-off among different performance requirements, particularly good regulation versus peak control action. The following weights offer a good compromise:

$$w_e(s) = \frac{1}{2}\frac{0.002s + 1}{0.002s} \tag{10}$$

$$w_u(s) = \frac{5 * 10^{-5}s}{10^{-7}s + 1} \tag{11}$$

The weight on the control error $w_e(s)$ was selected to be very large at low frequencies in order to get good tracking and regulation. It allows an amplification of high frequency noise at a factor of 2. This weight can approximately give a closed-loop bandwidth of $1/0.002 = 500 rad/s$. Note that an integrator is

included in $w_e(s)$ to get zero steady-state error. We may relax this requirement if we allow for a small, non–zero, steady-state error.

The weight on the control input $w_u(s)$ was chosen close to a differentiator to penalize fast changes and large overshoot in control input.

It should be pointed out that reference input r and weight on the control input $w_u(s)$ are not necessarily involved in the design since there are no specific requirements on tracking and control input. By not including neither r nor $w_u(s)$, then the following higher performance weight can be used:

$$w_e'(s) = \frac{1}{2}\frac{10^{-5}s + 1}{10^{-5}s} \tag{12}$$

Using this weight robust performance ($\mu_{RP} < 1$) can still be achieved, while obtaining acceptable control input under line voltage variations. However, the control input for reference input changes has very large peaks. This difference is caused by the transfer function $G_g(s)$ in the disturbance channel. Finally, it should be pointed-out that the weight on the control input $w_u(s)$ alone has little effect as the control input under line voltage variation is fine.

4.4 μ-optimal controller

By using the uncertainty description developed in section 4.2 and the performance weights of section 4.3, we get an uncertainty structure Δ with a scalar block (corresponding to the uncertainty) and a 2x2 block (corresponding to the performance). Using μ-toolbox[6], we obtained a 13rd-order μ-optimal controller with $\mu_{RP} = 0.9823$. Model reduction yielded a 6^{th} order controller with virtually no performance degradation ($\mu_{RP} = 0.9845 < 1$). The state space description of this reduced order controller is given in Appendix.

5 Simulation Results

The control system was simulated at four different operating points: $R_o = 45\Omega$, 19Ω, 17Ω and 13Ω. The time responses to unit step change in line voltage V_{ng} and reference input r are shown in Figure 7.

For the nominal case $R_o = 19\Omega$, the settling time is about 2 msec. for line voltage change and is less than 1 msec. for reference input change. The output responses are excellent. The control input response to line voltage change is also adequate. However the control input response to reference input change has an overshoot, that can reach values as high as 10, leading to implementation problems. Thus, the design was modified leading to the present value. If one wants to attenuate this overshoot further, more penalty on control input must be used and the performance requirements on the output must be relaxed accordingly. When the operating point moves to $R_o = 45\Omega$, the settling times are about doubled while the overshoot of the control action corresponding to a step disturbance at the input (modelling a sudden drop of the line voltage) decreases. When the operating point moves towards heavier loads, the responses are almost the same as the nominal, with the exception of the appearance of some chattering in both output and control input. This chattering becomes very severe when the load reaches $R_o = 13\Omega$ (note that this load is outside the range considered in our design).

It should be noted that simulations at different load conditions are used to estimate the load regulation performance. To get an exact evaluation, a nonlinear simulation of the SRC circuit is required. We have performed this simulation using P-Spice. The responses to reference input change and line voltage change are very similar to those obtained using a linear simulation (shown in Figure 7). The responses to load change also show a very good match. Due to the limited space, the nonlinear responses are not included here. They will be presented at the conference and can be obtained by contacting the authors.

Acknowledgements. This work was supported in part by NSF under grant ECS-9211169.

References

[1] Freeland, S., "An Introduction to the Principle and Features of Resonant Power Conversion," *Rockwell International Corporation–Autonetics ICBM Systems Division,* Anaheim, CA, 1988.

[2] Batarseh, I. and Lee, C. Q., "Steady–State Analysis of the Parallel Resonant Converter with LLCC-Type Commutation Network," *IEEE Trans. Power Electronics,* 6, 3, pp. 525–538, July 1991.

[3] Kassakian J. and Schlecht, M., "High Frequency High Density Converters for Distributed Power Supply Systems, *Proceedings of the IEEE,* 76, 4, April 1988.

[4] Siri, K., "Analysis of Resonant Converters and Control Approaches for Parallel Connected Converter Systems," *Ph.D. Dissertation,* University of Illinois, Chicago, July 1991.

[5] Vorperian, V., "Analysis of Resonant Converters," *Ph.D. Dissertation,* California Institute of Technology, May 1984.

[6] Balas, G. J. et al., "μ-Analysis and Synthesis Toolbox", April, 1991.

[7] Doyle, J. C., 1982, "Analysis of feedback systems with structured uncertainties," *IEE Proc., Pt. D,* **129**(6), 242-250.

[8] Lundstrom, P., S. Skogestad and Z.-Q. Wang, 1991 "Performance weight selection for H-infinity and mu-control method' *Transactions of the Institute of Measurement and Control,* **13**(5), 241-252.

[9] Lundstrom, P., S. Skogestad and Z.-Q. Wang, "Uncertainty weight selection for H-infinity and mu-control methods", *Proc. IEEE Conf. Decision Contr.*, Brighton, December, 1991.

[10] Wang, Z.-Q., S. Skogestad, "Robust controller design for uncertain time-delay systems", *Proc. of the 10th International Conference on Optimization and Analysis of Systems,* Sophia-Antipolis(France), June 9-12, 1992.

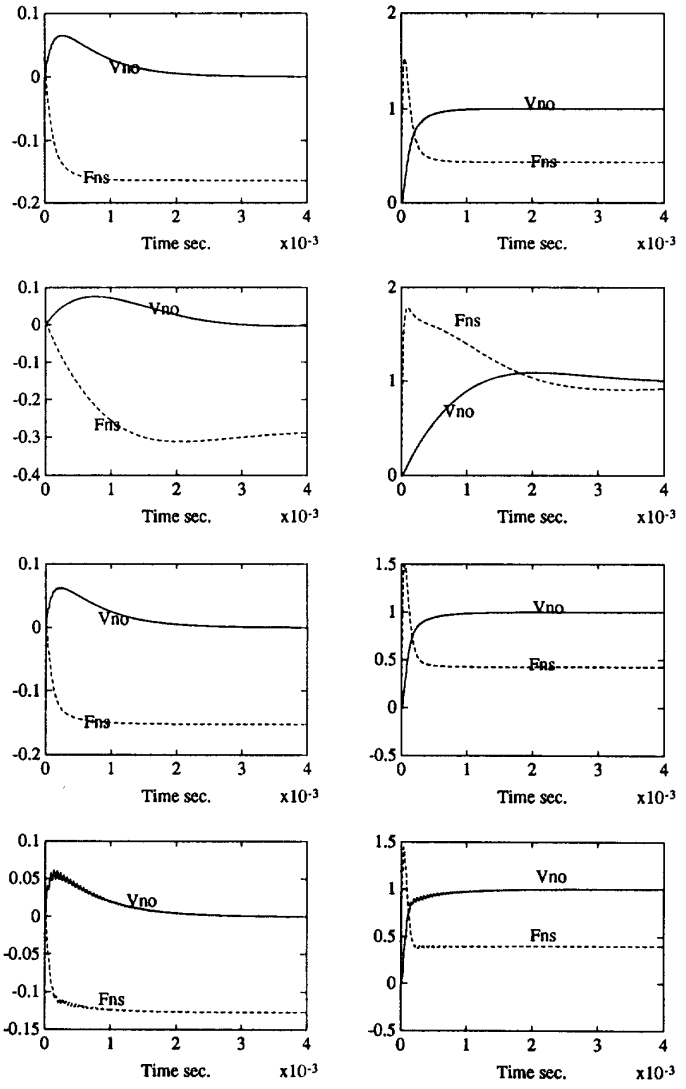

Figure 7: Simulation Results for $R_o = 19, 45, 17$ and 13Ω:
(a) Line Voltage Step Change. (b) Reference Input Step Change.

Appendix

The state space description of the reduced order controller is:

$$K = C_k(sI - A_k)^{-1}B_k + D_k$$

where

$$A_k = \begin{pmatrix} -1.3168e+6 & 6.1616e+4 & 2.9727e+5 & 5.8762e-3 & -1.1337e+5 & -2.9589e+4 \\ 0 & -1.5521e+3 & -1.6672e+5 & 4.8989e-4 & 1.4202e+4 & 4.0904e+3 \\ 0 & 1.5538e+5 & -3.4725e+4 & -2.4731e-3 & 3.9246e+4 & 1.0892e+4 \\ 0 & 0 & 0 & -1.0000e-3 & -5.2654e-3 & 3.8998e-4 \\ 0 & 0 & 0 & 0 & -4.2728e+4 & -2.2189e+4 \\ 0 & 0 & 0 & 0 & 0 & -7.6411e+3 \end{pmatrix},$$

$$B_k^T = (-153.51 \quad 38.575 \quad 56.637 \quad -50.427 \quad -278.14 \quad -49.935),$$

$$C_k = (189.56 \quad 34.243 \quad 17.456 \quad -50.427 \quad -244.77 \quad -103.71),$$

$$D_k = -3.8034e-3$$